

Automatic control of blood flow rate on the arterial-line side during cardiopulmonary bypass

Hideobu Takahashi, Takuya Kinoshita, Member, IEEE,
Zu Soh, Member, IEEE, and Toshio Tsuji, Member, IEEE

Abstract—The operation of the cardiopulmonary bypass (CPB) system requires skilled techniques and experience. Intraoperatively, the perfusionist needs to intermittently manipulate both of the occluders on the venous- and arterial-line sides to achieve the desired blood flow rates. To facilitate the occluder operation, we propose an automatic control system for the arterial-line side blood flow rate based on a dynamic model that addresses the relationship between the occluder operation and blood flow rate in the CPB system. The simulation results demonstrated that the proposed system was able to control the blood flow rate even when the estimation error of the model parameters was presented. Then, we implemented this control system in the CPB system and conducted an experiment to automatically control the arterial-line side blood flow rate. We confirmed that the blood flow rate on the arterial-line side could follow the manually operated venous-line side blood flow rate.

Clinical Relevance— The automatic blood flow rate control system for a cardiopulmonary bypass system, proposed in this paper, contributes to reducing the burden of occluder operation on a perfusionist.

I. INTRODUCTION

Cardiopulmonary bypass (CPB) devices temporarily replace heart and lung function to maintain systemic circulation during cardiac surgery. The CPB device developed by Gibbon [1] is widely implemented in clinical practice. CPB operations include maintaining blood flow, venous reservoir level, oxygen gas concentration, oxygen gas blood flow, and blood temperature; injecting cardioplegia fluid; monitoring biometrics and device information; and recording the operation. Faulty operation of blood flow rate control is dangerous because it can lead to circulatory disturbances and massive air emboli, resulting in serious clinical deterioration [2,3].

Initiation and weaning are the most important and difficult processes for the perfusionist operating the CPB. Because the perfusionist needs to operate three devices (the venous-line side occluder, the arterial-line side occluder, and the centrifugal pump) quickly and delicately to adjust blood flow rates to the desired target values. Performing this operation incorrectly will cause an air embolus [4] and alter the venous reservoir level in the hard shell. Since the venous reservoir level is equal to the blood volume in the patient's heart and lungs, an incorrect operation can lead to unintended blood pressure fluctuations, putting the patient at risk. Therefore, CPB initiation and weaning place a heavy psychological burden on the perfusionist. Accordingly, it would be useful to develop a device that helps automate blood flow rate adjustments.

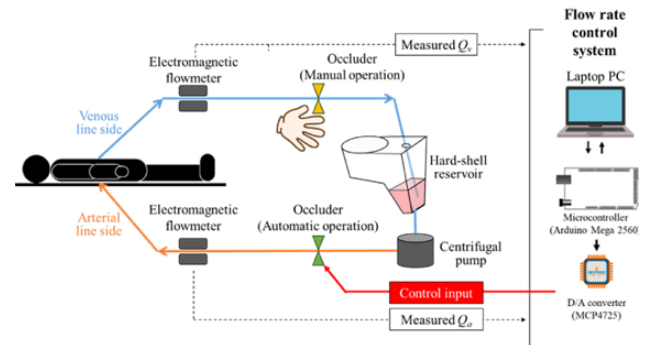


Fig. 1. Proposed automatic blood flow rate control system.

The purpose of this study is to develop an automatic blood flow rate control system for the arterial line incorporating our previous static model [5] that addresses the relationship between occluder operation and blood flow rate.

II. MATERIALS AND METHODS

A. Proposed blood flow rate control system

The configuration of the proposed automatic blood flow rate control system is described in this section. In the system, a venous-line side blood flow rate is controlled manually by a perfusionist, while the arterial-line side blood flow rate can be controlled automatically through the arterial-line side occluder of the CPB system in a way that it is equal to the manually controlled venous-line side blood flow rate.

1) The cardiopulmonary bypass system and the proposed system

Fig. 1 shows a diagram of the proposed control system integrated into a general CPB system. The system consisted of a hard-shell reservoir, a centrifugal pump, occluders to regulate blood flow rates, and electromagnetic flowmeters (Flow rate accuracy $\pm 5\%$). The components were connected using polyvinyl chloride tubes to form a closed circuit. The blood flow rate is determined by the output of the centrifugal pump and the occluder operation. In general, the output of the centrifugal pump is kept constant, and the blood flow rate is determined by occluder operations during the initiation and weaning of CPB.

The proposed blood flow rate control system shown in Fig. 1 was implemented in the arterial-line side occluder. Blood flow rate measured from the flowmeter was sampled by a microcontroller board with input to a laptop PC. This determines the amount of occluder operation by the proposed control system and outputs the control signal to the microcontroller board. The output control signal automatically controls the arterial-line-side occluder through a D/A converter.

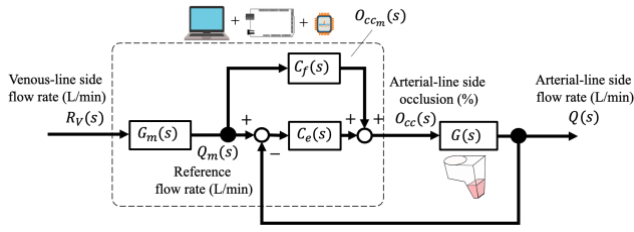


Fig. 2. Block diagram of cascaded blood flow rate control in the arterial line side.

2) The proposed control system

A block diagram of the control system is shown in Fig. 2. The control system is a two-degree of freedom control system that combine FF and FB controllers. In this figure, $R_v(s)$ represents the venous-line side blood flow rate (the target blood flow rate of the control system). $Q_m(s)$ is the desired reference trajectory tracking the target blood flow rate, $R_v(s)$. A user can specify $Q_m(s)$ by arbitrarily setting the reference model $G_m(s)$. The output $Q(s)$ is the arterial-line side blood flow rate from the control object $G(s)$, and the input $O_{cc}(s)$ is the control input to the occluder calculated in the microcontroller. First, the transfer function of the PID controller is defined as follows:

$$\begin{aligned} O_{cc}(s) &= C_e(s)E(s) + O_{ccm}(s) \\ E(s) &:= Q(s) - Q_m(s) \\ O_{ccm}(s) &:= C_f(s)Q_m(s), \end{aligned} \quad (1)$$

where $C_e(s)$ and $C_f(s)$ are the FB controller and the FF controller, respectively. $Q_m(s)$ shows the desired reference trajectory. The FB controller is designed as the following PID controller:

$$C_e(s) = K_P + \frac{K_I}{s} + K_D s, \quad (2)$$

where K_P denotes the proportional gain, K_I the integral gain, and K_D the derivative gain.

The FF controller $C_f(s)$ is designed using the inverse model of the controlled object model. In general, it is possible to calculate the ideal input, $O_{ccm}(s)$, using the inverse model of the controlled object model such that it tracks the desired reference trajectory $Q_m(s)$. In this case, $X_m(s)$ denotes the signal that realizes $Q_m(s)$. Based on the previous study [5], the static inverse model output $X_m(t)$ using $Q_m(t)$ can be expressed as follows:

$$X_m(t) = \frac{1}{K} \ln \left\{ \frac{1}{A \left(\frac{Q_0}{Q_m(t)} - 1 \right) R - \Delta R_0} + 1 \right\}, \quad (3)$$

where R represents the tube friction of the circuit without the occluder channel; ΔR_0 is the friction of occluder channel at 100% occlusion openness; Q_0 is the blood flow rate at 100% occlusion openness; and A and K are the constants.

The controlled object has the dynamic characteristics such as time-constant and time-delay. In this study, we use a model in which the time-delay is approximated by a first-order system. In addition, a filter is introduced to achieve the inverse model:

$$O_{ccm}(s) = \frac{(1 + Ts)(1 + Ls)}{(1 + T_f s)^2} X_m(s), \quad (4)$$

where L is the time-delay and T is the time constant. T_f is the filter coefficient, which is set arbitrarily by the user. From the above inverse model, we can design a feasible FF controller $C_f(s)$ that approximates the desired reference trajectory $Q_m(s)$.

If an exact controlled object model could be obtained and an inverse model could be designed without any approximation, then good control results could be expected using only $C_f(s)$. However, in an actual system, it is difficult to obtain an exact model, and it is difficult to calculate the inverse model without approximation. Thus, owing to modeling errors and other influences, $O_{ccm}(s)$ alone cannot track the reference trajectory $Q_m(s)$. Therefore, $O_{cc}(s)$ is calculated by correcting $O_{ccm}(s)$ to reduce the error using the PID controller (2). In this study, the pole placement method was used to calculate the PID gains.

B. Experiments

1) Numerical simulation

To verify the effectiveness of the proposed method, the results of the proposed control system were compared with those of the FB controller without the FF controller. We also evaluated the control results when the system parameters in $C_f(s)$ were different from the true values. The simulator consists of a step input, a reference model, a controller, and a controlled object model. The flow rates expressed by the step functions are input to the proposed control system. A controller (i) with the FF controller or (ii) without the FF controller is selected. The arterial-line side occlusion (%) automatically generated by the proposed control system is applied to the controlled object model (a simulated patient), and then the arterial-line side blood flow rate is fed back to the proposed control system.

First, to verify the effectiveness of the FF controller based on the dynamical inverse model, simulations were conducted for the proposed control system with and without the FF controller, and tracking accuracies were compared against the target blood flow rate input. It should be noted that the control system without the FF controller is a control system with an I-PD controller only, which is expressed by the following equation:

$$O_{cc}(s) = \frac{K_I}{s} E(s) - K_P Q(s) - K_D s Q(s). \quad (5)$$

The parameters of the control object model were set based on our previous study [5]. The input was varied in a staircase manner by adding uniform random numbers to the target blood flow rate, and this simulation is referred to as Simulation 1. The tracking accuracy of the arterial-line side blood flow rate Q (L/min) output from the control object model was evaluated by the mean absolute error of the blood flow rate per unit time using the following equation:

$$J = \frac{1}{N} \sum_{i=1}^N |Q_m(i) - Q(i)|, \quad (6)$$

where N represents the total number of samplings, $Q_m(i)$ is the desired reference blood flow rate, and $Q(i)$ is the output of the arterial-line side blood flow rate. To operate the proposed control system, it is necessary to estimate the parameters of the

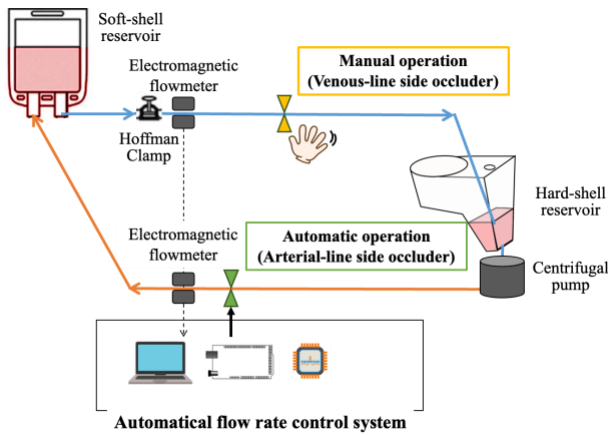


Fig. 3. Schematic drawing of the automatic blood flow rate control system for the simulation experiment.

static model (R, Q_0, A, K) and time constant (T) in advance; however, these parameters are expected to contain estimation errors. Therefore, we conducted simulations to verify the operation of the proposed control system against the parameter estimation error of the model. For each parameter, a normal random number with a mean of zero and a standard deviation of $P\%$ of the estimated value was added to the estimated value, and control systems with and without the FF controller were constructed. The target blood flow rate input was varied in a staircase manner, and the tracking accuracy of the arterial-line side blood flow rate Q (L/min) was evaluated using equation (6). This simulation is referred to as Simulation 2.

In Simulation 1, the input was varied in steps (0–33 s, 33–66 s, and 66–100 s). The target blood flow rate for each input interval was varied in uniform random numbers between 1.0 and 3.0 L/min. The sampling interval was set to $\Delta t = 0.01$ s, and the total measurement time was set to $st = 100$ s, i.e., $N = \frac{st}{\Delta t}$. The filter factor was set as $T_f = 0.2$ s, and σ as $\sigma = T + L$ where the time constant was $T = 1.95$ s with the time-delay $L = 0.5$ s. The time constant (T) here was estimated by calculating from $Q(t)$ using the inverse models, in which T was estimated by using the least-squares method. The parameters of the static model were set to $R = 0.013$ mmHg · min/L, $Q_0 = 2.9461$ L/min, $A = 0.0155$ L/mmHg·min, and $K = 0.104$ [5].

In Simulation 2, the standard deviation of normal random numbers was set to $P = 5, 10, 15,$ and 20% of each parameter value set in Simulation 1. In both simulations, the tracking accuracy of the control system with and without the FF controllers (equation (6)) was compared using the Wilcoxon signed-rank sum test. The significance level was set at $P < 0.05$. Simulations were performed using MATLAB R2019b, and statistical analysis was performed using IBM SPSS Statistics for Windows, version 22.0.

2) Simulation experiment

Fig. 3 shows the configuration of the system for the simulation experiment. This system consists of a CPB system and a proposed control system. The CPB system consisted of a hard-shell reservoir (HVR-4NFP; Senko Medical Instrument Mfg. Co. Ltd.) and a centrifugal pump (CX-SL45X; Terumo Cardiovascular Systems Corp. Tokyo, Japan). A pair of occluders to regulate blood flow rates (HAS-RH200; Senko

Medical Instrument Mfg. Co. Ltd. Tokyo, Japan) and electromagnetic flowmeters (FD-M5AT Ltd. Tokyo, Japan) were also used. The soft-shell reservoir was installed to simulate a patient (Fig. 3). The components of the CPB system were connected by polyvinyl chloride tubing, and the electromagnetic flowmeter and occluder were attached to the arterial-line side (3/8 inch tube) and the venous-line side (1/2 inch tube).

The operator manually controlled the venous-line side blood flow rate of the CPB system, while the proposed control system controlled the arterial-line side blood flow rate so that it was equal to the venous-line side blood flow rate using the model with the best tracking accuracies obtained from the simulation. Here, the measured venous-line side blood flow rate was sampled by an Arduino Mega 2560 microcontroller. The output of the model controlled the occluder through an MCP4725 D/A converter.

The glycerin solution used as the experimental fluid was prepared by adding glycerin to water. The glycerin solution (5 L) was stored in a hard-shell reservoir. The viscosity of the glycerin solution (2.84 mPa·s, 18.8°C) was measured by an oscillating viscometer (SV-10; A&D, Tokyo, Japan). The maximum flow rate was adjusted to 3.0 L/min for the venous- and arterial-line sides by a centrifugal pump and a Hoffman clamp. The venous- and arterial-line side flow rates were smoothed using a second-order Butterworth low-pass filter with a cutoff frequency of 5 Hz. Simultaneously, a camera was used to measure the fluid level in the hard-shell reservoir. Manual control was performed assuming initiation and weaning, which are difficult to operate. For initiation, the flow rate was increased from 0 to 3.0 L/min in 150 s. Then, the flow rate was increased to 3.0 L/min in 50 s. Next, the flow rate was maintained at 3.0 L/min for 50 s, followed by weaning. The weaning operation decreased the flow rate from 3.0 to 1.0 L/min at 150 s. After maintaining 1.0 L/min for 100 s, the flow rate was instantly decreased to 0 L/min and stopped.

III. RESULTS AND DISCUSSION

A. Numerical simulation

Figs. 4A and 4B show examples of results of Simulation 1 with and without the FF controller. During the period of constant blood flow rate, the reference blood flow rate and the output blood flow rate were almost the same for both cases, but when the blood flow rate changed, there was a difference in results. In the case without the FF controller, tracking accuracy deteriorated when the target blood flow rate changed. Tracking accuracies with and without the FF controller were compared, and the results demonstrated improved tracking accuracy with the FF controller ($p = 0.017$).

Fig. 5 shows the results of Simulation 2. Tracking accuracies were worse when the estimated parameter error was larger, regardless of the presence or absence of the FF controller. The comparison of the tracking accuracies demonstrated improved accuracies with the FF controller ($p < 0.05$) regardless of the estimated parameter error. This is because the response time required to achieve the target blood flow rate is smaller with the FF controller.

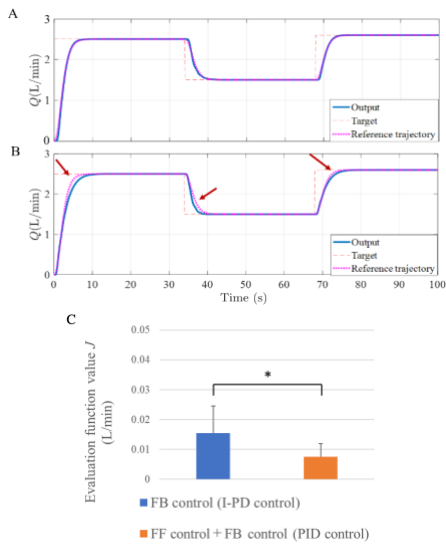


Fig. 4. Results of Simulation 1. In these examples, the target blood flow rate was varied in steps of 2.5 L/min, 1.5 L/min, and 2.6 L/min.

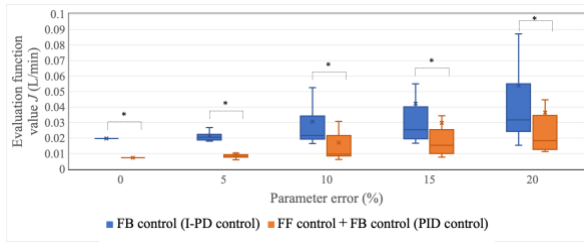


Fig. 5. Results of simulation 2. Box plots for the evaluation function values J against the parameter error using the control system with and without the FF controller.

B. Simulation experiment

Fig. 6A shows flow rate changes obtained from simulation experiments. Oscillations in the actual flow rate of the arterial-line side were observed during initiation (0–150 s) and weaning (225–360 s) when the flow rate was varied. During flow rate maintenance (150–225 s), the mean difference in flow rate between the venous- and arterial-line sides was 0.0096 ± 0.552 mL/min, and the 95% confidence interval included 0. The mean difference in flow rate between the venous- and arterial-line sides was 0.0043 ± 0.454 mL/min during flow rate maintenance (360–460 s), and the 95% confidence interval included 0. The correlation coefficient between flow on the venous-line side and flow on the arterial-line side was $r = 0.9877$ ($p < 0.05$). Therefore, we confirmed that the proposed system could match the flow rate of the venous-line side with that of the arterial-line side.

Fig. 6B shows the amount of occluder changes during the experiment. Although the manual controller (the venous-line side) did not change the amount of occlusion (mean $98.322 \pm 1.723\%$) during flow rate maintenance (150–200 s), the automatic controller (the arterial-line side) showed oscillations (mean $66.649 \pm 12.495\%$).

Fig. 6C shows the reservoir fluid levels. If the flow rate of the venous-line side by the manual controller is exactly the same as the flow rate of the arterial-line side by the proposed controller, the fluid level will be constant. Fig. 6C shows that the reservoir

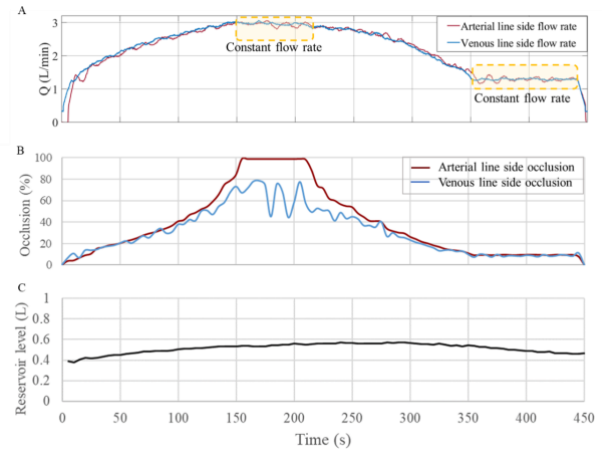


Fig. 6. Results of the simulation experiment. Results of the simulation experiment. Panel A shows change in flow rate. The green and blue lines show the flow rates of the venous- and arterial-line sides. Panel B shows changes in the openness (in percent) of the arterial- and venous-line side occluders. The green line represents the arterial-line side and the blue dotted line the venous-line side. Panel C shows the changes in the reservoir level.

level tended to increase until approximately 280 s, and then decreased until 450 s. The mean flow rate difference between the venous- and arterial-line sides was negligible when the flow rate was maintained (Fig. 6A). However, the flow rate of the arterial-line side was slightly lower than that of the venous-line side until approximately 280 s and slightly higher from approximately 280 s, which caused fluctuation of the reservoir levels. To minimize the reservoir level fluctuation, it is necessary to directly control the reservoir level, which should be examined in future research.

IV. CONCLUSIONS

In this study, we developed an automatic control system for the arterial-line side blood flow rate to reduce the burden of occluder operation during CPB. Simulation experiments showed that the system could stably maintain the target flow rate during CPB. Therefore, the proposed system has the potential to automate occluder operation of the arterial-line during CPB initiation and weaning. In the future, we plan to develop an additional control system to stabilize the reservoir level.

REFERENCES

- [1] J. H. Gibbon, Jr, "Application of a mechanical heart and lung apparatus to cardiac surgery," *Minn. Med.*, vol. 37, no. 3, pp. 171–185, March 1954.
- [2] J. R. Utley, "Techniques for avoiding neurologic injury during adult cardiac surgery," *J. Cardiothorac. Vasc. Anesth.*, vol. 10, no. 1, pp. 38–43, January 1996.
- [3] N. I. Mills and J. I. Ochsner, "Massive air embolism during cardiopulmonary bypass. Causes, prevention, and management," *J. Thorac. Cardiovasc. Surg.*, vol. 80, pp. 708–717, November 1980.
- [4] M. Frank, K. Dino, and S. Christoph, "Evaluation of attention, perception, and stress levels of clinical cardiovascular perfusionists during cardiac operations a pilot study," *Perfusion*, vol. 34, no. 7, pp. 544–551, October 2019.
- [5] H. Takahashi, S. Zu, and T. Tsuji, "Steady-state model of pressure-flow characteristics modulated by occluders in cardiopulmonary bypass systems," *IEEE Access*, vol. 8, pp. 220962–220972, December 2020.